Characterization of the Tryptophan Residues of *Escherechia coli* Alkaline Phosphatase by Phosphorescence and Optically Detected Magnetic Resonance Spectroscopy[†]

Sanjib Ghosh,[‡] Ajay Misra, Andrzej Ozarowski, Christina Stuart,[§] and August H. Maki*

Department of Chemistry, University of California at Davis, One Shields Avenue, Davis, California 95616

Received July 19, 2001

ABSTRACT: The phosphorescence and zero field optically detected magnetic resonance (ODMR) of the tryptophan (Trp) residues of alkaline phosphatase from *Escherichia coli* are examined. Each Trp is resolved optically and identified with the aid of the W220Y mutant and the terbium complex of the apoenzyme. Trp[109], known from earlier work to be the source of room-temperature phosphorescence (RTP), emits a highly resolved low-temperature phosphorescence (LTP) spectrum and has the narrowest ODMR bands observed thus far from any protein site, revealing a uniquely homogeneous local environment. The decay kinetics of Trp[109] at 1.2 K reveals that the major triplet population (70%) undergoes inefficient crystallike spin−lattice relaxation by direct interaction with lattice phonons, the remainder being relaxed efficiently by local disorder modes. The latter population is smaller than is typical for protein sites, suggesting an unusual degree of local rigidity and order consistent with the long-lived RTP. Trp[220] emits a broader LTP spectrum originating to the blue of Trp[109]. It has typically broad ODMR bands consistent with local heterogeneity. The LTP of Trp[268] has an ill-defined origin blue shifted relative to Trp[220] and ODMR frequencies consistent with a greater degree of solvent exposure. Trp[268] has noticeable dispersion of its decay kinetics, consistent with quenching at the triplet level by a nearby disulfide residue.

Escherechia coli alkaline phosphatase (AP)[1] is an extensively studied metalloenzyme whose functional form consists of a homodimer with an approximate mass of 94 kDa (*1*) that binds two Zn^{2+} and one Mg^{2+} in each of two active sites. Phosphate is tightly bound by the active enzyme but is released upon removal of the metal ions (*2*). Each AP monomer contains three tryptophan (Trp) residues at positions 109, 220, and 268. AP has received much attention in that it emits room-temperature Trp phosphorescence (RTP) (*3*) having a lifetime of ca. 2 s, the longest thus far reported (*4*). The long-lived emission has been assigned to Trp[109] (*5−8*) that is buried deep in the hydrophobic core of AP. Solvent-exposed Trp residues, on the other hand, have RTP lifetimes of ca. 1 ms in carefully deoxygenated solution (*9*). Studies of Trp (*10*) and *N*-acetyltryptophan amide (*9*) suggest that increasing RTP lifetime is correlated with increasing solvent viscosity. It is now generally accepted (*3*) that long RTP lifetimes of Trp are associated with residues that are bound in rigid local protein environments.

Although only relatively few Trp residues (those that are located in buried, rigid local environments) can be studied readily using RTP, nearly all Trp residues emit phosphorescence at low temperature. Their origins often can be resolved because of the relatively narrow emission bands that characterize Trp low-temperature phosphorescence (LTP). The narrowness of the LTP bands, in contrast with the poorly resolved fluorescence of tryptophan, is attributed to the smaller excited-state dipole moment in the case of the triplet (*11*). The LTP of Trp residues buried in hydrophobic regions within proteins is generally red-shifted relative to solvent-exposed residues, and it is better resolved since buried environments are usually more highly structured, i.e., homogeneous (*12*). Specific interactions with polar residues, however, can result in blue shifted origins for buried Trps (*13, 14*).

Optically detected magnetic resonance (ODMR) studies carried out on the excited triplet state of Trp residues in proteins (*15−18*) indicate that the bandwidth of the ODMR signals correlates well with the homogeneity of the local environment. Buried residues in homogeneous protein environments yield narrow ODMR signals. In addition, red-shifted phosphorescence origins correlate with reduced values of $D − E$ (*13, 15*), where D and E are the triplet state zero field splitting (zfs) parameters (*19*). The structure of the

[1] Abbreviations: AP, *E. coli* alkaline phosphatase; apoAP, metal-depleted AP; Cys, cysteine; *D* and *E*, triplet state zero field splitting parameters; EED, electron−electron dipolar; EEDOR, electron−electron double resonance; EG, ethylene glycol; EPPS, *N*-(2-hydroxyethyl)-piperazine-*N'*-(3-propanesulfonic acid); hwhm, half of the bandwidth at half its maximum intensity; isc, intersystem crossing; LTP, low-temperature phosphorescence; MIDP, microwave-induced delayed phosphorescence; ODMR, optically detected magnetic resonance; RNase T1, ribonuclease T1 from *Aspergillus oryzae*; RTP, room-temperature phosphorescence; slr, spin−lattice relaxation; TbAP, apoAP containing excess terbium; Tris, tris(hydroxymethyl)aminomethane; Trp, tryptophan; Tyr, tyrosine; zfs, zero field splittings.
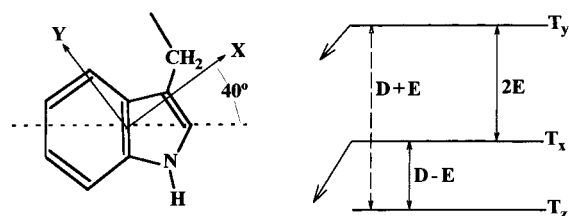
FIGURE 1: Structure of the indole chromophore of Trp showing the orientation of the zfs principal axes and the zero field energy level diagram. The prominent ODMR transitions between triplet sublevels, T_i, are indicated with solid double-headed arrows, while that made visible using EEDOR is labeled with the dashed double-headed arrow. Diagonal arrows indicate the radiative sublevels.

tryptophanyl side chain with the location of the zfs principal axes is shown in Figure 1, along with the zero field energy level diagram.

The objective of this work is to use the intrinsic high resolution of LTP and ODMR spectroscopy of Trp to characterize the individual residues of AP. We expected that Trp[109], identified as the source of the uniquely long-lived RTP, would reveal the presence of a very homogeneous environment at cryogenic temperature. With the aid of the mutant W220Y AP that contains only Trp[109] and Trp[268] and from selective Trp quenching by terbium substituted at the metal sites, we are able to characterize Trp[109] and Trp[220] with respect to phosphorescence origin, bandwidth, and triplet state properties. We find that Trp[109] is located in an extremely homogeneous microenvironment, yielding a highly structured LTP spectrum and the narrowest ODMR bands of any Trp residue thus far observed in proteins. Furthermore, disorder mode enhancement of spin−lattice relaxation (20−22) is less efficient than is typically found at protein sites as would be expected for a highly structured and rigid environment. Trp[220] has the properties of a partially solvent exposed residue with bandwidths typical for an inhomogeneous microenvironment. Trp[268] in W220Y AP phosphorescence is found to be weak with a wide distribution of lifetimes consistent with excited-state quenching at the triplet level.

MATERIALS AND METHODS

AP was a product of Sigma (type III, chromatographically purified suspension in 2.5 M $(NH_4)_2SO_4$, activity 43.7 u/mg of protein). AP was exchanged into 100 mM Tris buffer containing, in addition, 1 mM Na_2HPO_4, 0.1 mM $MgCl_2$, and 0.1 mM $ZnCl_2$, using Centricon 30 filter centrifugation at 5000g and 4 °C. Ethylene glycol (EG) was added to 30 vol % as cryoprotectant for low-temperature measurements. The final concentration of AP in our samples is about 2.5×10^{-4} M. W220Y AP was a generous gift from Prof. Ari Gafni, Department of Biological Chemistry, University of Michigan. We obtained samples in 10 mM EPPS buffer, pH 7.5, containing 100 mM NaCl, 1 mM Na_2HPO_4, 1 mM $MgCl_2$, and 1 mM $ZnCl_2$. The construction of W220Y AP has been described previously (8). Samples were concentrated by centrifugation as described above, 30 vol % of EG added, and then frozen in liquid N_2 for low-temperature measurements. The final concentration of W220Y AP is about 3×10^{-5} M in our samples. AP with terbium substitution at the metal sites (TbAP) was obtained by first preparing metal-depleted AP (apoAP) following the method of Bosron et al. (2) using the metal chelator, 8-hydroxy-

quinoline-5-sulfonic acid (Aldrich). ApoAP was washed with three exchanges of metal-free Tris. Tris buffer containing 10 mM $TbCl_3$ was added and the solution incubated for 30 min prior to washing the TbAP twice with metal free buffer. The entire procedure was carried out by refrigerated (4 °C) centrifugation at 5000g using a Centricon 30 filter.

Samples (30−50 μL) are contained in a 2 mm inside diameter Suprasil quartz tube held inside a copper helix terminating a coaxial stainless steel microwave transmission line. This structure is inserted into a stainless steel dewar with quartz optical windows in which the sample temperature can be held at 77 K (boiling N_2 temperature), 4.2 K (immersed in boiling He), or 1.2 K (immersed in vacuum-pumped He) for LTP and ODMR measurements that are made in the absence of an applied steady magnetic field. The sample is excited by a 100 W high-pressure Hg lamp whose output is filtered through a 0.1 m monochromator. Glass filters are used as required to further limit the excitation band. Phosphorescence is observed through a rotating sector with a delay period of ca. 1 ms and monitored through a 1 m monochromator with a dispersion of 0.8 nm/mm. Details of the phosphorescence and ODMR spectrometer that employs photon counting to enhance sensitivity have been described previously (23, 24). Center frequencies (ν_0) and bandwidths ($\nu_{1/2}$, half the bandwidth at half-maximum intensity, hwhm) of the ODMR bands (assumed Gaussian shape) are determined by analysis of phosphorescence responses, obtained by sweeping the microwave frequency slowly through the zero field resonance band, using algorithms developed previously for steady-state ODMR (23) and for delayed ODMR (25). These algorithms correct for band distortions caused by rapid passage effects. The highest frequency ($D + E$) ODMR band is observed using electron−electron double resonance (EEDOR) (16), simultaneously saturating the low-frequency ($D − E$) band (Figure 1). The individual kinetic parameters of the triplet state sublevels are obtained by global analysis of microwave-induced delayed phosphorescence (MIDP) (26) data sets using a previously described procedure (24). These are comprised of the sublevel decay constants, k_i, the spin−lattice relaxation (slr) rate constants W_{ij}, the relative intersystem crossing (isc) rates, P_i, and relative radiative rate constants R_{ix} ($=k_i^r/k_x^r$). i, $j = x, y, z$ label the principal zero field magnetic axes of the indole chromophore of Trp, where z is normal to the molecular plane and x is directed nearly normal to the C═C bond of the five-membered ring (15−18, 27), Figure 1. Decay kinetics are obtained using a mechanical shutter in the excitation path with a closing time of 1 ms. Tryptophan LTP lifetimes at 4.2 K are obtained in the following manner. The decay of tyrosine (Tyr) LTP is recorded with wavelength selection just to the blue of the Trp emission. This decay is weighted by its contribution to the steady-state phosphorescence intensity at the 0,0-band peak of Trp and subtracted from the overall LTP decay at this wavelength. The tyrosine contribution is readily assessed since its phosphorescence presents a broad, unstructured background in contrast with the highly resolved bands of Trp. The residual LTP, attributed to Trp, is fitted to a single exponential using least-squares minimization. Tryptophan LTP decay at 4.2 K and at 77 K is known to be exponential over at least 3 decades (15, 16), while tyrosine decays nonexponentially at these temperatures (28, 29).
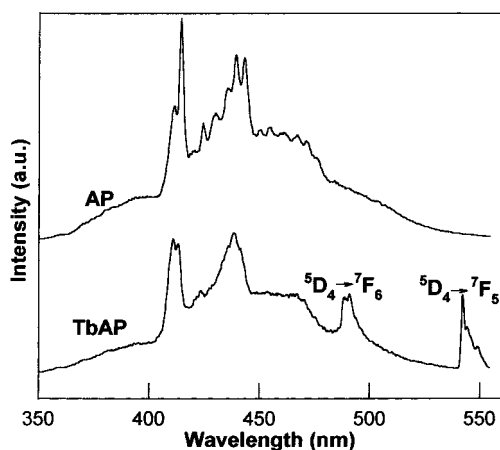
FIGURE 2: Phosphorescence spectra of AP and TbAP. Samples are dissolved (2.5×10^{-4} M) in 30% (v/v) EG$-$buffer glass at 4.2 K. Samples are excited at 280 nm, and the emission bandwidth is 1 nm. The sample is viewed through a rotating can phosphoroscope with delay time of 1 ms. Two sensitized terbium emission bands are indicated in the TbAP spectrum. Phosphorescence intensity is normalized at 411.4 nm.
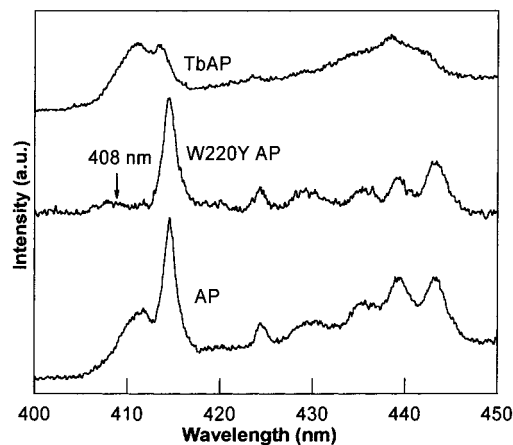

FIGURE 3: High-resolution phosphorescence of AP, W220Y AP, and TbAP at 1.2 K. Samples are as described in the Figure 2 caption but W220Y AP is 3.0×10^{-5} M. Samples are excited at 280 nm and viewed through the phosphoroscope using 0.5 nm emission bandwidth. Arrow indicates wavelength monitored when observing ODMR of Trp[268] in W220Y AP.

A measurement of the effectiveness of disorder mode relaxation of the triplet sublevels of Trp[109] at 1.2 K is carried out with W220Y AP since this mutant has a negligible amount of interfering Trp phosphorescence at 414.5 nm, the 0,0-band peak wavelength of Trp[109] (see below). The decay of Tyr phosphorescence is recorded at 1.2 K, weighted as described above, and subtracted from the LTP decay obtained at 414.5 nm. The resulting nonexponential decay, attributed to Trp[109], is analyzed according to the previously described method (*21, 22*) utilizing the kinetic parameters of Trp[109] as determined by global analysis of MIDP (*24, 26*).

RESULTS

Phosphorescence. The LTP of AP observed at 4.2 K is shown in Figure 2. The spectrum contains a broad underlying band originating near 350 nm that is assigned to Tyr. Superimposed on this background is a highly structured tryptophan spectrum that has two resolved 0,0-bands peaking at 411.4 and 414.5 nm, respectively. The spectrum of TbAP, seen below that of AP in Figure 2, shows that the Trp residue emitting at 414.5 nm is severely quenched relative to that with the 411.4 nm origin. The 414.5 nm origin will be assigned to Trp[109] (see below). Some quenching of Tyr also is evident (the emission intensity is normalized at 411.4 nm). Sensitized emission characteristic of Tb is also present in this spectrum. Measurement at 4.2 K of the decay kinetics of the Tb peak of TbAP at 542.4 nm reveals major components the order of 20 and 200 ms (data not shown) that can only be consistent with energy transfer from long-lived donor states. The lifetime of the excited $^5D_4$ state of Tb in TbCl$_3$ was measured at 4.2 K in an aqueous EG glass and found to be in the 2$-$3 ms range. Similar effects of energy transfer also are observed at 77 K, but the spectra (not shown) are not so well resolved because of thermal broadening. The central portions of the Trp LTP spectra of AP and TbAP observed at 1.2 K are presented in Figure 3 at higher resolution. Also included is the LTP of W220Y AP. Immediately apparent from the 0,0-band region of the AP emission is the difference in bandwidth of the 411.4 and 414.5 nm origins. The apparent width of the 414.5 nm band

is only 40 cm^{-1}, hwhm, in contrast with the 411.4 nm band that has a more typical value (for protein sites) of 150 cm^{-1}. The W220Y AP mutant is missing the LTP band at 411.4 nm, thus identifying this origin to be from Trp[220]. The narrow 414.5 nm band is present at the same location indicating that the mutation at position 220 has no apparent effect on the environment of Trp[109]. Monitoring the LTP of W220Y AP at 408 nm (arrow) produces (at 1.2 K) slow-passage ODMR signals and triplet state kinetic properties from MIDP measurements that are distinct from those obtained when monitoring the 411.4 or 414.5 bands of AP (see below). We attribute these properties to Trp[268]. Although it is not observable in Figure 3, we note here that the W220Y mutation causes a substantial increase in the underlying Tyr phosphorescence intensity.

Optically Detected Magnetic Resonance. The slow passage ODMR transitions of AP that are found in the $D - E$ frequency region of Trp are shown in Figure 4. The $D - E$ transition occurs between the T_z (longest lived and nonradiative) and T_x (shortest lived and most radiative) sublevels and is (without a known exception to date) the narrowest of the three ODMR bands of Trp (*15, 16*). The Trp[109] ODMR bands are found in both AP and W220Y AP by optically selecting the 414.5 nm 0,0-band with slits set for a narrow band-pass. The unusually narrow ODMR band has a doublet structure in both samples. A broader ODMR band, assigned to Trp[220] is observed in AP by monitoring the LTP at 411.4 nm, and a band, assigned to Trp[268], is found observing the W220Y AP emission at 408 nm (Figure 3). ODMR bands also were observed from these residues in the 2E region and from Trp[109] and Trp[220] in the $D + E$ region using EEDOR. These data were analyzed using algorithms described previously (*20, 22*); the zfs data are reported in Table 1. ODMR signals of Tyr (not reported) occur in different frequency ranges and do not interfere with those of Trp (*15, 16*). No ODMR signals are detected in samples of TbAP at 1.2 K. In contrast with AP and W220Y AP, the LTP decay kinetics of TbAP at 1.2 K are indistinguishable from those measured at 4.2 K. Bound Tb apparently induces efficient slr in the triplet states so that the spin alignment at 1.2 K is lost. The mechanism is likely to involve interaction between the triplet
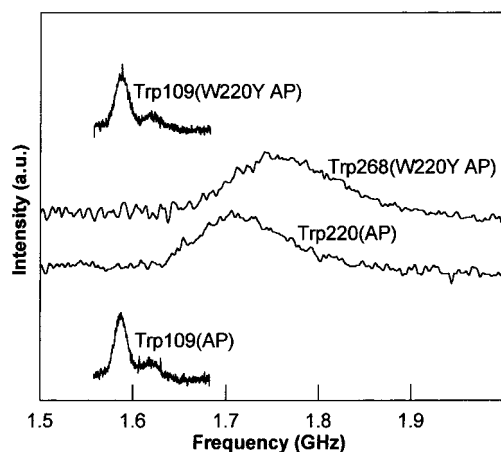
FIGURE 4: Slow passage $D - E$ ODMR transitions of Trp in AP and W220Y AP at 1.2 K. The Trp[109] band is observed monitoring the 0,0-band at 414.5 nm with 0.5 nm bandwidth. Trp[220] is observed monitoring the 0,0-band at 411.4 nm with 1 nm bandwidth. Trp[268] is monitored at 408 nm with 2 nm bandwidth. Sweep rate is 2.67 MHz/s for Trp[109], 4.5 MHz/s for Trp[220], and 30 MHz/s for Trp[268]. Steady-state ODMR is employed for Trp[109] and Trp[220], while delay ODMR is used for Trp[268] to enhance sensitivity (sweep begins at 1.4 GHz after 5 s delay). Signal averaging is employed for 40 cycles, except for Trp[268], where 20 cycles are used.

states of W and a fluctuating magnetic field set up by the $J = 6$ ground state of Tb.

Triplet Sublevel Kinetic Properties of Trp Residues. Global analysis of MIDP data sets was carried out (24) yielding the kinetic data reported in Table 2. The microwave sweep was restricted to the ODMR band of a residue and the decay was monitored in its 0,0-band (reported in Table 1) to select the residue and to minimize signal contamination. The MIDP signals attributed to Trp[268], observed in W220Y AP monitoring the LTP at 408 nm, are characterized by a wide dispersion of lifetimes and cannot be analyzed globally in terms of three sublevel lifetimes (24).

Disorder Mode Relaxation of Trp[109]. The deconvolution of the Trp[109] contribution to the phosphorescence decay of W220Y AP into components predicted from global MIDP analysis (24), which arises from a triplet state population undergoing slow (crystallike) spin−lattice relaxation (slr), and a second population undergoing rapid spin−lattice relaxation is shown in Figure 5. The rapidly relaxing population of triplet states is coupled to low-energy tunneling states (30, 31) that are associated with structural disorder (20). We have found previously (21, 22) that for tryptophan the latter population decays primarily as a single exponential with the average triplet state lifetime since the slr rate

constants exceed the individual k_i which become averaged. Thus, as seen in Figure 5, the observed decay is fitted well by the weighted sum of a single exponential and the calculated nonexponential decay of the population with slow slr. The lack of a significant population of triplet states with slr rate constants comparable to the larger k_i yields this bimodal distribution that is readily analyzed as demonstrated in Figure 5. The rate constant found for the rapidly relaxing population ($k_{av} = 0.153$ s^{-1}) should correspond to that of Trp[109] measured at higher temperature (4.2 K, Table 2) when the entire population undergoes averaging by rapid slr (0.166 s^{-1}). The difference is somewhat larger than we have found in previous examples (20, 21) and could result from the large contribution of Tyr (37%) to the LTP intensity at 414.5 nm. The ratio of the initial intensity of slowly relaxing to rapidly relaxing triplet states is converted to their population ratio using an equation derived previously (20). The result is that 30% of the Trp[109] population undergoes rapid slr induced by disorder modes.

DISCUSSION

Phosphorescence. The LTP of AP is characterized by two well-resolved 0,0-bands of Trp superimposed on a relatively intense broad emission band assigned to Tyr. Of the two Trp origin bands at 411.4 and 414.5 nm, the latter is extremely narrow, about 40 cm^{-1} hwhm, comparable to the Trp[59] 0,0-band of ribonuclease T1 from *Aspergillus oryzae* (RNase T1) (13), a buried residue. The LTP band at 414.5 nm is selectively quenched in TbAP. The kinetics of the Tb emission demonstrates that energy transfer originates from a long-lived triplet state. On the other hand RTP of AP, known to originate from Trp[109], is quenched in TbAP (32) by energy transfer from the triplet state as verified by kinetics measurements. On this basis, we assign the 0,0-band at 414.5 nm to Trp[109]. Catalytic activity of AP requires the presence of Zn^{2+} at metal binding site M1 (33) while Zn^{2+} and Mg^{2+} bound at M2 and M3, respectively, could have either a structural (33) or cocatalytic function (34, 35). We do not know for certain which of these metal sites contain Tb in our sample of TbAP, but previous work (32) demonstrates that triplet energy transfer to Tb occurs with a single bound Tb per AP monomer. Trp[109] is the closest tryptophan residue to the metal sites. The distances between its indole ring center (midpoint of the $C_\delta - C_\epsilon$ bond) and M1, M2, and M3 are 13.7, 9.7, and 9.3 Å, respectively. These distances are obtained from atomic coordinates deposited in the Brookhaven Protein Data Bank (35). Schlyer et al. (32) conclude that the Trp[109] triplet state transfers energy predominantly to Tb

Table 1: Spectroscopic Properties of Tryptophan Residues of AP[a]

| sample and residue | λ0,0 (nm) | $D - E$ | | 2E | | $D + E$ | | D (GHz) | E (GHz) |
		ν_0 (GHz)	$\nu_{1/2}$ (MHz)	ν_0 (GHz)	$\nu_{1/2}$ (MHz)	ν_0 (GHz)	$\nu_{1/2}$ (MHz)		
AP, Trp109	414.5 site I	1.583(3)	7.0(5)	2.768(8)	18(1)	4.344(1)	13(1)	2.964	1.382
	414.5 site II	1.61(2)	11(1)	2.704(5)	20(1)			2.96	1.35
AP, Trp220	411.4	1.675(5)	43(2)	2.63(6)	94(12)	4.29(1)	53(3)	2.98	1.31
W220Y AP, Trp109	414.5 site I	1.583(9)	7(2)						
	414.5 site II	1.613(3)	11(2)						
W220Y AP, Trp268	408	1.723(1)	44(3)	2.60(6)	136(25)			3.02	1.30

[a] D and E are the zfs parameters of the tryptophan residue indicated whose phosphorescence is monitored at the 0,0-band peak, $\lambda_{0,0}$. Excitation is at 280 nm. ODMR transitions are observed in the absence of an applied magnetic field at the $D - E$, 2E, and $D + E$ frequencies given by ν_0 with bandwidth $\nu_{1/2}$ defined as the half-bandwidth at half-maximum intensity. The $D + E$ transition is observed using EEDOR by saturating the $D - E$ band. Estimated error in the last digit is given in brackets.

Table 2: Kinetic and Radiative Parameters of the Trp[109] and Trp[220] Residues in AP[a]

sample and residue	τ (s)	k_x (s^{-1})	k_y (s^{-1})	k_z (s^{-1})	R_{yx}	R_{zx}	W_{xy} (s^{-1})	W_{xz} (s^{-1})	W_{yz} (s^{-1})	P_x	P_y	P_z
AP, Trp109	5.9	0.39(1)	0.106(7)	0.004(5)	0.00(1)	0.00(1)	0.033(5)	0.030(8)	0.0402(9)	0.60	0.30	0.10
AP, Trp220	5.95	0.390(9)	0.113(4)	0.000(3)	0.065(6)	0.036(9)	0.004(3)	0.045(4)	0.0402(4)	0.43	0.48	0.09
W220Y AP, Trp109	6.02	0.39(2)	0.101(9)	0.003(7)	0.00(1)	0.00(2)	0.050(7)	0.03(1)	0.051(1)	0.61	0.30	0.09

[a] All measurements are made monitoring the 0,0-band of the Trp residue using MIDP with these data obtained at 1.2 K and analyzed globally as described in the text. k_i is the sublevel decay constant, R_{ix} is the relative radiative rate constant, and P_i is the relative intersystem crossing rate constant of the T_i sublevel ($i = x, y, z$). The W_{ij} are slr rate constants. τ is the lifetime component attributed to tryptophan, obtained by elimination of the tyrosine contribution, this measurement being made at 4.2 K. The sample is excited at 280 nm. The estimated error in the last digit is given in parentheses while the estimated error of P_x and P_y is ±0.03.
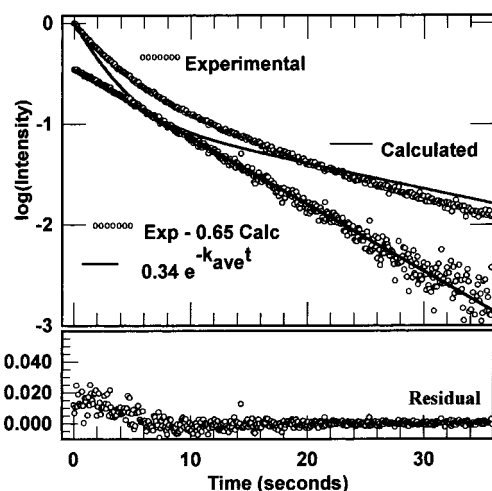

FIGURE 5: Analysis of Trp[109] phosphorescence decay kinetics from W220Y AP at 1.2 K. Phosphorescence is monitored at 414.5 nm using 1 nm band-pass. Tyrosine decay, monitored at 394 nm, weighted by its contribution to the intensity at 414.5 nm is subtracted to obtain the Trp decay, labeled "Experimental". These data are plotted with an initial intensity of 1. The predicted decay of the population with slow slr, obtained from global analysis of the Trp[109] MIDP data, is labeled "Calculated" and plotted with an initial intensity of 1. The latter is weighted by 0.65 and subtracted from "Experimental" to produce the data labeled "Exp − 0.65 Calc". These data are fitted to a single exponential, "0.34 exp-$(−k_{av}t)$" using a nonlinear least-squares procedure. The residuals are shown in the panel below. The minor initial transient that appears in the residuals (1−2% of the initial intensity) may include some Trp[268] phosphorescence. The preexponential factor of the single exponential decay, 0.34, differs from the fraction of the triplet state population that is relaxed by disorder modes, 0.30, since this population has negligible spin alignment, while the population that decays nonexponentially is spin-aligned. This correction is discussed in ref *21*.

bound in M2 or M3 by an electron exchange (Dexter) mechanism.

In the mutant W220Y AP, the 0,0-band at 411.4 nm is missing (Figure 3), allowing us to assign this origin to Trp[220]. There is no observed change in the 0,0-band wavelength or bandwidth of Trp[109], indicating that this residue is little affected by the W220Y mutation. The far greater bandwidth of the 0,0-band of Trp[220] points to a more heterogeneous microenvironment than that experienced by Trp[109]. Its location at 411.4 nm is consistent with a partially solvent-exposed environment. In low-temperature glasses, solvent-exposed Trp residues such as found in short peptides have 0,0-bands that peak at ca. 408 nm, while those buried in hydrophobic regions are narrower with a peak in the 412−415 nm range (*15, 36*). The substantial increase in Tyr phosphorescence in W220Y AP relative to AP could reflect the proximity of Trp[220] and Tyr[234] in the crystal structure (*35*). Energy transfer to Trp[220] would be likely to quench

Tyr[234] emission in AP, while, in W220Y AP, both Tyr[234] and Tyr[220] would emit, there being no Trp acceptor nearby.

Although Trp[268] does not appear to have a prominent 0,0-band, it contributes nonetheless to the LTP at 408 nm and is characterized by short as well as long lifetime MIDP components, consistent with triplet state quenching of this residue. We have encountered similar dispersion of lifetime from Trp sites located near a cystine residue in ODMR measurements of snake venom neurotoxins (*37*). Disulfides are the only known intrinsic quenchers of Trp phosphorescence in proteins (*38*). LTP lifetime shortening is attributed to electron transfer from Trp to cystine (*39, 40*), and its dispersion is accounted for by a distribution of Trp−disulfide interactions frozen into the low-temperature glass. The proximity of the Cys[286]−Cys[336] disulfide to Trp[268] is revealed in the crystal structure of AP (*35*). The distance found between the midpoint of this disulfide bond and the midpoint of the $C_\delta−C_\epsilon$ bond of Trp[268] is 6.0 Å.

Optically Detected Magnetic Resonance. It is interesting that the ODMR signals of Trp[109] in both AP and W220Y AP appear as two bands, labeled site I (major) and site II (minor) in Table 1. Their splitting, ca. 30 MHz, is too large to ascribe to ^{14}N quadrupole and hyperfine interactions in zero field (*41*). We believe that the site I and site II bands originate from distinct AP conformations that involve slightly different Trp[109] interactions with the surrounding protein matrix. These conformations appear to survive unaltered in the W220Y mutation. The sites are too subtly different to be resolved in the phosphorescence spectrum (Figure 3), however. It is possible that the minor band (site II) represents the contribution of AP without a complete complement of bound metal, i.e., it could lack one of the Mg^{2+}. The ODMR bands of Trp[109] in site I are 2−3 times narrower than any thus far observed in protein sites (Figure 4, Table 1). The $D − E$ bandwidth of 7 MHz, hwhm, indicates that the environment is unusually homogeneous. Having one of the narrowest ODMR bands previously observed, Trp[99], a buried residue of *E. coli* tryptophan repressor, has a $D − E$ bandwidth of 18 MHz, hwhm (*42*), and other buried residues have $D − E$ bandwidths the order of 20 MHz, hwhm (*14, 15*). Care should be exercised when comparing ODMR bandwidths quoted in the literature. The bandwidths in this work are given as hwhm, as are those in some relatively recent work referenced here, refs *14, 21−25, 46*, and *47*. In earlier work, refs *13, 15−18, 28*, and *42*, the bandwidths are given as the *full* width at half the maximum intensity. In addition, the bandwidths from the earlier work are subject to greater error since distortion of the band shape by rapid passage effects is not fully accounted for in some cases. Trp[109], site II, although not so homogeneous as site I nonetheless is extremely well defined. It is notable that the

RTP of AP has been found to decay nonexponentially (*43*) and that analysis by the maximum entropy method (*44*) produces two distinct lifetime peaks of 1920 ms (major) and 380 ms (minor). This behavior was attributed to the existence of (at least) two discrete structures that are unable to interconvert on the RTP time scale. We suggest that the nonexponential RTP decay may arise from the conformations that are resolved as site I and site II in the ODMR spectra.

In addition to well-resolved red-shifted LTP spectra, Trp residues buried in nonpolar protein sites are characterized by a large value of the zfs E parameter (*15*). In this regard, Trp^{109} in site I is a typical buried residue with an E value among the largest observed for Trp. Trp^{109} in site I of AP, with $E = 1.382$ GHz, is comparable to Trp^{99} of *E. coli* tryptophan repressor (*42*) ($E = 1.36$ GHz), azurin B (*15*) ($E = 1.39$ GHz), and Trp^{108} of hen egg-white lysozyme ($E = 1.36$ GHz) (*15*). Tryptophan, as well as small Trp peptides in which indole is in contact with polar solvent, have $E \sim 1.24$ GHz (*15*). Trp^{220} of AP ($E = 1.31$ GHz) is in a less hydrophobic environment but cannot be characterized as a solvent exposed residue. Its bandwidths (Table 1) place it in a moderately heterogeneous location but not so heterogeneous as tryptophan and small tryptophan-containing peptides in polar glasses that have $D - E$ bandwidths in the range, 60−70 MHz, hwhm. Trp^{268} is located in a similarly inhomogeneous environment based on ODMR bandwidths (Table 1). The zfs parameters, larger D and smaller E, suggest that the environment is more polar than that of Trp^{220} possibly due to greater solvent exposure..

Global analysis of the MIDP data (Table 2) reveals a typical pattern of sublevel decay constants for both Trp^{109} and Trp^{220}, with $k_x > k_y > k_z$ and $k_z = 0$, within experimental error. k_x is larger than that of tryptophan in a polar glass, 0.309 s^{-1} (*24*), and is typical for buried tryptophan residues in proteins (*14*). The pattern of slr for the slowly relaxing population (see below) is quite typical for Trp^{220}, with $W_{xy} < W_{xz}, W_{yz}$, but Trp^{109} is unusual in that there is essentially no sublevel specificity for slr. Trp^{109} also differs from Trp^{220} in its isc pattern. $P_x < P_y$ is observed for tryptophan in aqueous glass, whereas $P_x > P_y$ (and enhancement of k_x) is found often for tryptophan where it is subjected to interactions that reduce the planar symmetry of the aromatic residue (*45−47*).

Spin−Lattice Relaxation Induced by Disorder Modes. It is well established that slr in *crystalline* matrixes is the result of energy exchange between the spins and lattice phonons either through direct or through Raman processes (*48*). At 1.2 K the density of phonons is very small and Raman processes are ineffective, leaving slr to occur only by the direct process. Slr is thus quite inefficient because of the low density of resonant phonon states, leading to W_{ij} in the $10^{-2}−10^{-1}$ s^{-1} range for typical aromatic triplet states in crystalline hosts (*22, 49*). This is the range of the slr rate constants found for the Trp residues in AP from analysis of the MIDP data (Table 2). It can be concluded, therefore, that the population responsible for the MIDP responses undergoes slr by direct interaction with matrix phonons; i.e., slr is crystallike for this population.

Slr occurs much more efficiently in triplet states that are dissolved in disordered solids such as glasses, even at the lowest temperatures. Gradl and Friedrich proposed (*20*) that enhancement of slr is caused by the coupling of low-energy disorder modes to the spins through modulation of the electron−electron dipolar (EED) interaction. The EED interaction is the source of the zfs in Trp and similar aromatic molecules. Sufficient disorder modes, modeled as two-level systems (*30, 31*), are active even at 1.2 K and efficiently relax spins to which they are coupled. Disorder modes, by their very nature, are not present in truly crystalline material. We have found (*21, 22*) that the triplet states of tryptophan in a frozen glass at 1.2 K can be described in terms of two populations; one undergoes slow slr and contributes to ODMR and MIDP, while the other undergoes rapid slr (relative to the triplet sublevel lifetimes) and is ODMR and MIDP silent. The latter population is coupled to active disorder modes, and its LTP decays, except for a weak initial transient, as a single exponential with the average decay constant of the triplet sublevels, $k_{av} = \frac{1}{3}(k_x + k_y + k_z)$. Analysis (*21, 22*) of the LTP decay kinetics at 1.2 K allows us to determine their relative populations in the sample. As part of our characterization of the triplet states of AP, we were particularly interested in determining the efficiency of disorder mode relaxation of Trp^{109} that is located in an unusually homogeneous and rigid protein environment. To the extent that this environment can be described as crystalline, we felt that disorder mode activity should be suppressed. Thus, we expected that Trp^{109} would display a smaller population that undergoes rapid slr than a Trp residue located in a more typical protein environment. The fraction of the triplet population of tryptophan in 30% and 40% (v/v) EG−water glass that undergoes rapid slr at 1.2 K is 0.36 (*21*), which is smaller than most protein sites that we have analyzed recently, although for Trp^{59} of RNase T1 it is comparable (0.38).

From the analysis shown in Figure 5, we determined that the fraction of the Trp^{109} population that is subject to rapid slr is 0.30. Because site II contribution to the phosphorescence intensity at 414.5 nm is minor on the basis of its relative ODMR intensity (Fig. 4), this distribution is effectively that of site I. We have analyzed the LTP decays (1.2 K) of Trp in a number of protein sites and find much variation in the efficiency of disorder mode-induced slr. In most cases the fractional population undergoing rapid slr is near 0.5, suggesting that typical protein sites exhibit greater disorder mode activity than either Trp in EG−water glass or Trp^{109} in AP. The observation that the population of tryptophan in EG−water glass undergoing rapid slr is smaller than in many protein environments, even though the latter are more ordered (narrower ODMR and phosphorescence bands, in general) suggests that it is the rigidity of the environment rather than its homogeneity that correlates with disorder mode activity. However, the presence of a detectable, although relatively small population of Trp^{109} triplet states in AP that is subject to disorder mode relaxation implies that the environment lacks perfect crystalline order. On the other hand, when compared with other protein environments, it has one of the lowest populations subject to disorder mode relaxation. This is consistent with its long phosphorescence lifetime at room temperature that is attributed to its rigid local environment.

SUMMARY

The tryptophan residues of *E. coli* alkaline phosphatase (AP) are investigated at low temperature using phosphores-

cence and ODMR spectroscopy. Of particular interest are the properties of Trp[109] triplet state that is the source of the unusually long-lived room-temperature phosphorescence (RTP). This residue is identified from its selective quenching by terbium bound at the metal sites and comparison with the W220Y AP mutant. Trp[109] is found to have the narrowest ODMR bands of any Trp residue thus far investigated (7 MHz, hwhm for the $D - E$ transition), revealing an unusually homogeneous environment. The ODMR bandwidths of Trp[220] and Trp[268], on the other hand, are broad and typical for protein sites. The low-temperature spin−lattice relaxation (slr) of the triplet state of Trp[109] also is studied and reveals that 30% of its population undergoes rapid slr via interaction with disorder modes, while the remaining population is characterized by slow slr with rate constants typical of triplet states in crystalline sites. The population that relaxes rapidly by coupling with disorder modes is smaller than is found in most protein sites under these conditions (ca. 50%, work to be published) but is not much less than the rapidly relaxing population of tryptophan in low-temperature aqueous glass (36%). The latter has broader ODMR lines than do typical Trp sites in proteins, suggesting that site rigidity rather than homogeneity per se should be associated with inefficient relaxation by disorder modes as it is with long-lived RTP.

ACKNOWLEDGMENT

REFERENCES

1. Coleman, J. E. (1992) *Annu. Rev. Biophys. Biomol. Struct. 21*, 441−483.
2. Bosron, W. F., Anderson, R. A., Falk, M. C., Kennedy, F. S., and Vallee, B. L. (1977) *Biochemistry 16*, 610−614.
3. Schaurte, J. A., Steel, D. G., and Gafni, A. (1997) *Methods Enzymol. 278*, 49−71.
4. Vanderkooi, J. M., Calhoun, D. B., and Englander, S. W. (1987) *Science 236*, 568−569.
5. Domanus, J., Strambini, G. B., and Galley, W. C. (1980) *Photochem. Photobiol. 31*, 15−21.
6. Strambini, G. B., and Gabellieri, E. (1990) *Photochem. Photobiol. 51*, 643−648.
7. Mersol, J. V., Steel, D. G., and Gafni, A. (1991) *Biochemistry 30*, 668−675.
8. Fischer, C. J., Schauerte, J. A., Wisser, K. C., Gafni, A., and Steel, D. G. (2000) *Biochemistry 39*, 1455−1461.
9. Strambini, G. B., and Gonnelli, M. (1995) *J. Am. Chem. Soc. 117*, 17646−17651.
10. Strambini, G. B., and Gonnelli, M. (1985) *Chem. Phys. Lett. 115*, 196−200.
11. Hahn, D. K., and Callis, P. R. (1997) *J. Phys. Chem. A 101*, 2686−2691.
12. Galley, W. C., and Purkey, R. M. (1970) *Proc. Natl. Acad. Sci. U.S.A. 67*, 1116−1121.
13. Hershberger, M. V., Maki, A. H., and Galley, W. C. (1980) *Biochemistry 19*, 2204−2209.
14. Ozarowski, A., Barry, J. K., Matthews, K. S., and Maki, A. H. (1999) *Biochemistry 38*, 6715−6722.
15. Kwiram, A. L. (1982) in *Triplet State ODMR Spectroscopy. Techniques and Applications to Biophysical Systems* (Clarke, R. H., Ed.) pp 427−478, John Wiley and Sons, New York.
16. Maki, A. H. (1984) in *Biological Magnetic Resonance* (Berliner, L. J., and Reuben, J., Eds.) Vol. 6, pp 187−294, Plenum Press, New York.
17. Hoff, A. J. (1994) *Methods Enzymol. 227*, 290−330.
18. Maki, A. H. (1995) *Methods Enzymol. 246*, 610−638.
19. McGlynn, S. P., Azumi, T., and Kinoshita, M. (1969) *Molecular Spectroscopy of the Triplet State*, Prentice-Hall, Englewood Cliffs, NJ.
20. Gradl, G., and Friedrich, J. (1987) *Phys. Rev. B 35*, 4915−4921.
21. Wu, J. Q., Ozarowski, A., and Maki, A. H. (1997) *J. Phys. Chem. A 101*, 6177−6183.
22. Ozarowski, A. Wu, J. Q., and Maki, A. H. (1998) *Chem. Phys. Lett. 286*, 433−438.
23. Wu, J. Q., Ozarowski, A., and Maki, A. H. (1996) *J. Magn. Reson. Ser. A 119*, 82−89.
24. Ozarowski, A., Wu, J. Q., and Maki, A. H. (1996) *J. Magn. Reson. Ser. A 121*, 178−186.
25. Wu, J. Q., Ozarowski, A., Davis, S. K., and Maki, A. H. (1996) *J. Phys. Chem. 100*, 11496−11503.
26. Antheunis, D. A., Schmidt, J., and van der Waals, J. H. (1970) *Chem. Phys. Lett. 6*, 255−258..
27. Smith, C. A., and Maki, A. H. (1993) *J. Phys. Chem. 97*, 997−1003.
28. Ugurbil, K., Maki, A. H., and Bersohn, R. (1977) *Biochemistry 16*, 901−907.
29. Ghosh, S., Zang, L.-H., and Maki, A. H. (1988) *Biochemistry 27*, 7816−7820.
30. Anderson, P. W., Halperin, B. I., and Varma, C. M. (1972) *Philos. Mag. 25*, 1−9.
31. Phillips, W. A. (1972) *J. Low Temp. Phys. 7*, 351−360.
32. Schlyer, B. D., Steel, D. G., and Gafni, A. (1995) *J. Biol. Chem. 270*, 22890−22894.
33. Simpson, R. T., and Vallee, B. L. (1968) *Biochemistry 7*, 4343−4350.
34. Vallee, B. L., and Auld, D. S. (1993) *Biochemistry 32*, 6493−6500.
35. Stec, B., Holtz, K. M., and Kantrowitz, E. R. (2000) *J. Mol. Biol. 299*, 1303−1311.
36. Purkey, R. M., and Galley, W. C. (1970) *Biochemistry 9*, 3569−3575.
37. Schlyer, B. D., Lau, E., and Maki, A. H. (1992) *Biochemistry 31*, 4375−4383.
38. Li, Z., and Galley, W. C. (1989) *Biophys. J. 56*, 353−360.
39. Bent, D. V., and Hayon, E. (1974) *J. Am. Chem. Soc. 97*, 2612−2619.
40. Vanderkooi, J., Englander, S. W., Papp, S., Wright, W. W., and Owen, C. S. (1990) *Proc. Natl. Acad. Sci. U.S.A. 87*, 5099−5103.
41. Dinse, K. P., and Winscom, C. J. (1982) in *Triplet State ODMR Spectroscopy. Techniques and Applications to Biophysical Systems* (Clarke, R. H., Ed.) pp 83−136, John Wiley and Sons, New York.
42. Burns, L. E., and Maki, A. H. (1994) *J. Fluoresc. 4*, 217−226.
43. Schlyer, B. D., Schauerte, J. A., Steel, D. G., and Gafni A. (1994) *Biophys. J. 67*, 1192−1202.
44. Livesey, A. K., and Brochon, J. C. (1987) *Biophys. J. 52*, 693−706.
45. El-Sayed, M. A., Moomaw, W. R., and Chodak, J. B. (1973) *Chem. Phys. Lett. 20*, 11−16.
46. Misra, A., Ozarowski, A., Casas-Finet, J. R., and Maki, A. H. (2000) *Biochemistry 39*, 13772−13780.
47. Maki, A. H., Ozarowski, A., Misra, A. Urbaneja, M. A., and Casas-Finet, J. R. (2001) *Biochemistry 40,* 1403−1412.
48. Bowman, M. K., and Kevan, L. (1979) in *Time Domain Electron Spin Resonance* (Kevan, L., and Schwartz, R. N., Eds.) pp 67−105, John Wiley and Sons, New York.
49. Ghosh, S., Weers, J., Petrin, M., and Maki, A. H. (1984) *Chem. Phys. Lett. 108*, 87−93.